

Experimental Evaluation of High-Frequency Magnetization Characteristics of Core Materials

Aditya Raj
Electrical Engineering Dept.
Indian Institute of Science
Bangalore, India
adityaraj@iisc.ac.in

Syed Shahjahan Ahmad
Electrical Engineering Dept.
Indian Institute of Science
Bangalore, India
shahjahans@iisc.ac.in

G Narayanan
Electrical Engineering Dept.
Indian Institute of Science
Bangalore, India
gnar@iisc.ac.in

Abstract—Aircraft and many other on-board applications require compact electric motor drives having high power densities. A typical motor drive includes an electrical machine controlled by a power-electronic converter. Ferromagnetic materials form an important part of such machines and integrated magnetics in power converters. Hence the knowledge of such materials at operating conditions of frequency and flux density is crucial in the electromagnetic and thermal design of such systems. The information in manufacturers' datasheets is limited and typically available at conventional frequencies like 50 Hz. However, operating frequencies in such motor drives can extend upto hundreds and thousands of Hz. Hence, in-house characterization of magnetic materials becomes necessary over the frequency range of interest. In this paper, two SiFe steels- 50C600 and 50C800 are characterized over a frequency range of 333 Hz to 1000 Hz, and upto flux densities of around 1.5 T. Experimental B-H loops are obtained at different frequencies and compared. Detailed procedure for evaluation of magnetization and core-loss curves from multiple B-H loops is provided. Core-losses at working levels of flux-densities are observed to be much higher at higher frequencies. The experimental data obtained, can be used in the design and analysis of magnetic structures fabricated using such materials.

Index Terms—Aircraft, B-H curve, loss curve, SiFe steel, 50C600, 50C800

I. INTRODUCTION

Design of electrical machines intended for aircrafts has severe dimensional constraints. Hence, the power density of current electrical machines needs to be increased by a factor greater than 2 [1]. Higher torque or higher speed is needed to achieve high power density [1]. High torque can be achieved by magnetic loading at high flux densities, or, by electrical loading at higher current densities [2]. Higher current densities lead to more power losses in conductors and thus pose thermal constraints. Due to this, the torque density of Permanent Magnet (PM) motors usually does not exceed 50 Nm/L [1]. Hence, the use of high magnetic loading is one of the possible ways to enhance torque density. This however requires proper selection of magnetic material in the design stage. Power density can also be enhanced by higher speed at same torque [1]. This requires the magnetic loading to be done at higher frequencies. As an example, a frequency range of 360 Hz to 800 Hz is often used in wound field synchronous generators (WFSGs) inside the aircrafts [3]- [7].

Further, any industrial motor drive requires power converters for efficient control of speed and torque. These power converters are switched at high frequencies upto kHz and MHz range in order to reduce the size requirement of filter inductor and/ or coupling transformer. Hence these magnetic components require low-loss core materials like Mn-Zn ferrite [9].

Proper selection of magnetic materials with low loss and high saturation flux densities is required in all such applications. This requires the knowledge of magnetic characteristics of prospective materials under operating conditions of frequency and flux density [8]. The datasheets of magnetic materials usually specify this information at frequencies like 50 Hz only [9], [10]. Hence there is a need to characterize the magnetic materials under desired conditions.

Magnetic materials may be broadly classified as conventional and non-conventional. Conventional magnetic materials include- SiFe, CoFe, NiFe, whereas non-conventional materials include- amorphous, nano-crystalline, SMC [2] [11]- [12]. Magnetic saturation and iron losses are typical parameters of magnetic materials [12]. Comparison of the materials in context of electrical machines is discussed in [2], [11]- [12]. A material selection guide is presented with characteristics at 50 Hz and 400 Hz [11]. A new comparison parameter: PB2 is also introduced to compare both magnetization and loss parameters. Experimental performance comparisons have also been done on a 5 kW, 1500 rpm, 8-pole PMSM [2]. Representative magnetic materials from each category of magnetic material is investigated. PMSM designed using CoFe alloy- Vacoflux 50 is reported to have high saturation flux-density, low loss, and higher power to mass ratio (kW/kg) than the PMSM designed using SiFe alloy - M19. However, the price of Vacoflux 50 is thirty times higher than M19 [2]. Hence CoFe alloys are limited to aircraft and space applications [2], [11]. Permendur is one such alloy manufactured by Hitachi for aircrafts [13].

Si-Fe is most popular among electrical machines [11]. M19 is widely used in PMSMs for commercial electric vehicles [2]. SiFe also comes next to CoFe in terms of magnetic saturation

TABLE I
DETAILS OF THE LAMINATIONS UNDER TEST

Core	Mass density (kg/m ³)	Iron loss at 1.5 T, 50 Hz (W/kg)	B at 5000 At/m (T)
50C600	7750	6	1.66
50C800	7800	8	1.7

and is much cheaper [2]. More Si is being introduced in the chemical composition recently. Magnetic characteristics of a SiFe steel with 6.5 % Si is compared with CoFe steel over frequency range of 1 to 5 kHz [14]. 6.5 % SiFe is reported to be better in terms of weight and efficiency for aircraft starter/genretaor application.

Si-Fe steels like M36 and 65C600 are characterized over frequency range of 1 Hz to 5 kHz in [8]. In this paper, two fully processed cold rolled non-oriented (CRNO) steels (mid. grade) are considered- 50C600 and 50C800. These materials are quite cost-effective, and find applications in medium rotating machines and in power transformers [10]. The details of the materials under test from its datasheet [10] are given in Table-I. Both the materials have a sheet thickness of 0.5 mm. The B-H loops, B-H curves, and core-loss curves of the two materials over a frequency range of 333 Hz to 1000 Hz and upto a flux density of 1.5 T are experimentally obtained and discussed.

II. EXPERIMENTAL PROCEDURE

The procedure adopted for magnetic characterization is similar to the one described in [8] [16], and is depicted in Fig. 1. Further details of the process along with the experimental setup are discussed next.

A. Sample preparation

The magnetic core laminates used for experimental magnetic characterization could be of different geometries. In an Epstein frame (IEC 60404-2) [17], [19], four rectangular strips of the magnetic material under test are assembled into a square geometry; multiple such squares are stacked together and tested. Instead of four rectangular strips, a single sheet is used in single-sheet tester (IEC 60404-3) [19]. These geometries consist of sharp corners along the flux path. Hence the flux density may become non-uniform along the flux path.

In this paper, toroidal strips of the magnetic material are used, following the ring specimen method (IEC 60404-6) [8] [18] [19] to ensure uniform cross-sectional area. Further, both magnetic materials are cut into toroids of outer diameter (OD) 100 mm and inner diameter (ID) 90 mm. The ratio of OD to ID being around 1.11 helps maintain the flux density uniform across the cross-section of the core [18] [19]. Ten laminates of 0.5 mm thickness each are stacked together to realize a stack height of 5 mm, as shown in Fig. 2(a).

The stack is insulated; primary and secondary coils are then wound over the insulated stack. The primary coil provides the necessary magnetomotive force (mmf) for measuring the B-H loop, while the secondary coil is used to sense the induced emf. Both coils have 50 turns each. The thickness of primary coil should depend on the maximum current it should carry; here SWG-19 wire is used. The thickness of secondary coil could be very low as this is open-circuited (SWG-27 is used here). The secondary coil is wound inside the primary coil and is closer to the core. This ensures low leakage in the secondary winding, and the induced emf across the secondary coil truly represents the time variation of core flux density. Fig. 2(b) shows the wound core with primary and secondary coil terminals.

B. Power source requirements

As mentioned earlier, the magnetic characteristics of the two materials are desired over a frequency range of 333 Hz to 1000 Hz, and upto a flux density (B_{max}) of 1.5 T. If a sinusoidally varying flux-density with peak value of B_{max} at the maximum frequency ω_{max} is to be produced inside a toroidal core with a cross-sectional area of A_ϕ , wound with a primary coil of N_p turns, then the required peak value of sinusoidal voltage is given by RHS of (1).

$$V_{rat} \geq N_p \cdot A_\phi \cdot B_{max} \cdot \omega_{max} \quad (1)$$

The primary coil is usually energized using a linear power amplifier [8] [15]. The voltage rating of such an amplifier V_{rat} should be greater than RHS of (1), considering resistive and leakage impedance drops. Based on RHS of (1) and dimensions of the core, it can be seen that the magnetic material samples used here require about 12 V to produce B_{max} of 1.5 T at 1000 Hz. The amplifier used in this paper is rated for peak sinusoidal voltage of 70 V [8], which is more than adequate for the given purpose. Since the peak sinusoidal current rating of the amplifier used is 10 A [8], H_{max} of up to 1,600 AT/m can be produced in the magnetic core by this experimental arrangement, as suggested by (2), where l_ϕ is the perimeter of the core.

$$I_{rat} \geq H_{max} \cdot \frac{l_\phi}{N_p} \quad (2)$$

C. Requirement of closed loop operation

For proper magnetic characterization of the material, the flux-density inside the core needs to vary sinusoidally between $+B_{max}$ and $-B_{max}$ at the desired frequency. This can be ensured if the secondary induced voltage is sinusoidal at the given frequency. This is achieved through closed-loop operation as indicated in Fig. 1. The measured open-circuit secondary voltage is compared against the desired sinusoidal reference; the error is fed to an error amplifier, whose output feeds the linear power amplifier. Proper design of error amplifier ensures that the core flux density and induced emf vary sinusoidally, even though the excitation current is non-

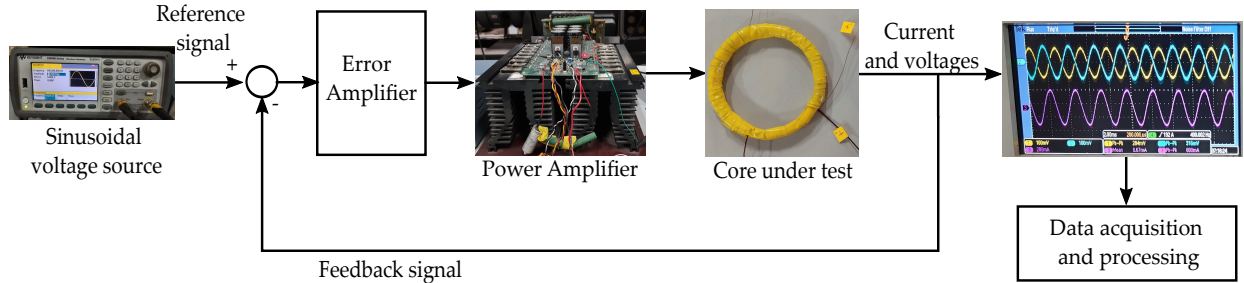


Fig. 1. Process of magnetic characterization using ring-specimen method

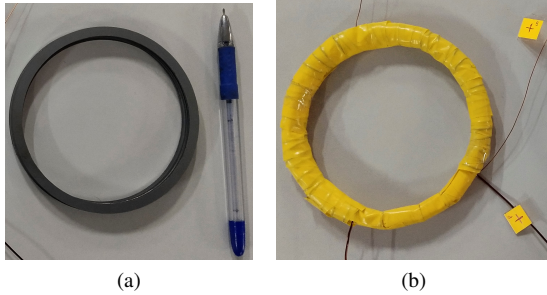


Fig. 2. 50C600 lamination (a) before winding (b) after winding

sinusoidal, and could even be peaky [16], on account of magnetic saturation.

D. Experimental setup

The complete experimental setup for characterization is shown in Fig. 3. A function generator (model no. 33500B, make- Keysight) generates the reference sinusoidal voltage. The reference signal along with the error between the reference and output signals gets amplified with the linear power amplifier, and is fed to the primary coil. Current probe powered with TCPA300 amplifier is used to sense the primary current. The induced emf from the secondary is sensed using a 200 MHz passive voltage probe (P2220). The primary current and induced secondary voltage are observed during runtime in DSO (DPO2024B), and therefrom acquired in a digital computer for further processing.

E. B-H loop measurement

The induced secondary voltage $e(t)$ and primary current $i(t)$ are acquired in a digital computer. $e(t)$ is numerically integrated with respect to time in an offline manner using trapezoidal method in software. This gives the flux linkage $\psi(t)$ according to (3). $B(t)$ and corresponding $H(t)$ are computed from $\psi(t)$ and $i(t)$ respectively by using (4) and (5).

$$\psi(t) = \int_0^t e(\tau) d\tau \quad (3)$$

$$B(t) = \frac{1}{N_p \cdot A_c} \cdot \frac{e(t)}{\omega} \quad (4)$$

$$H(t) = \frac{N_p \cdot i(t)}{l_\phi} \quad (5)$$

The measured B-H loops for the two materials at different frequencies and peak flux-densities are presented in the next section.

III. EXPERIMENTAL RESULTS

The experimental B-H loops for the two laminations 50C600 and 50C800, are obtained for a frequency range of 333 Hz to 1000 Hz. The B-H curves and loss curves at each frequency are therefrom obtained and demonstrated.

A. Measured B-H loops

The sample under test is excited with sinusoidal voltages of multiple amplitudes at each frequency of interest (excitation current and induced emf waveforms are not shown). In this way, a family of B-H loops corresponding to different peak flux-densities is obtained for each frequency. The B-H loops for 50C600 are shown in Fig. 4(a)-(c) at 400 Hz, 800 Hz, and 1000 Hz respectively. Similar B-H loops are shown for 50C800 in Fig. 5(a)-(c). It can be observed that for each frequency, the B-H loops are elliptical at lower values of peak flux density B_{max} . At higher values of B_{max} , the loops become S-shaped. Further, the B-H loops at higher frequencies are more towards oval shape and enclose larger area inside them. B-H loops at similar values of peak flux-density are compared at 400 Hz, 800 Hz, and 1000 Hz for each of the two materials. This is shown in Fig. 6(a)-(b), and discussed in a later section.

B. Magnetization curves

The flux densities corresponding to H_{max} for different B-H loops are joined together to get the B-H curve for that particular frequency. These B-H curves are shown in Fig. 7(a)-(d) for 50C600 and 50C800 over a frequency range of 333 Hz to 1000 Hz. It can be observed that the initial slope of the curve i.e., initial permeability gradually reduces at higher frequencies. However, the knee-point of the curve i.e., the flux density at which the saturation sets in the core, also increases at higher frequencies.

C. Core loss characteristics

The energy lost in the core in each cycle of magnetization and demagnetization can be determined from the area of each B-H loop. The procedure for core-loss evaluation is illustrated in Fig. 8. It shows two B-H loops measured for 50C600 at 1000 Hz. The smaller loop has a flux-density of 0.54 T at peak field intensity. Its area as shown in dark grey is evaluated to be

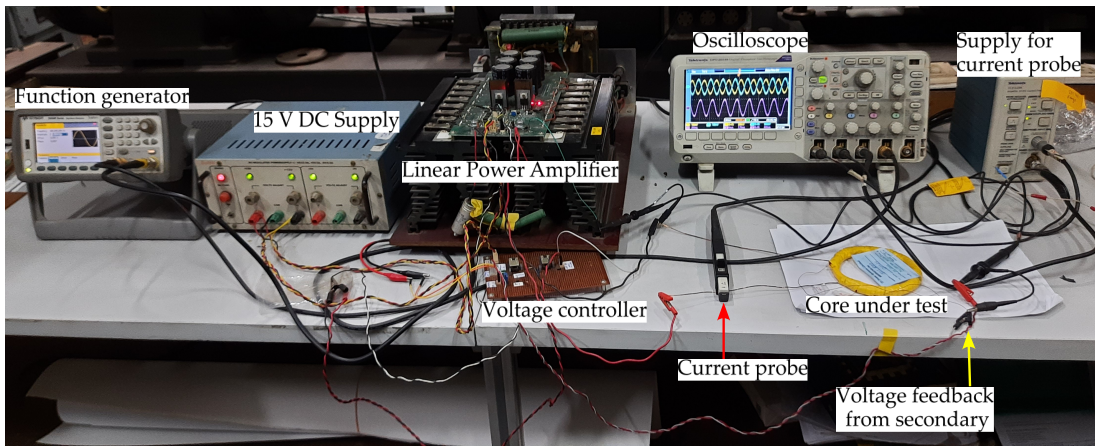


Fig. 3. Experimental setup for magnetic characterization

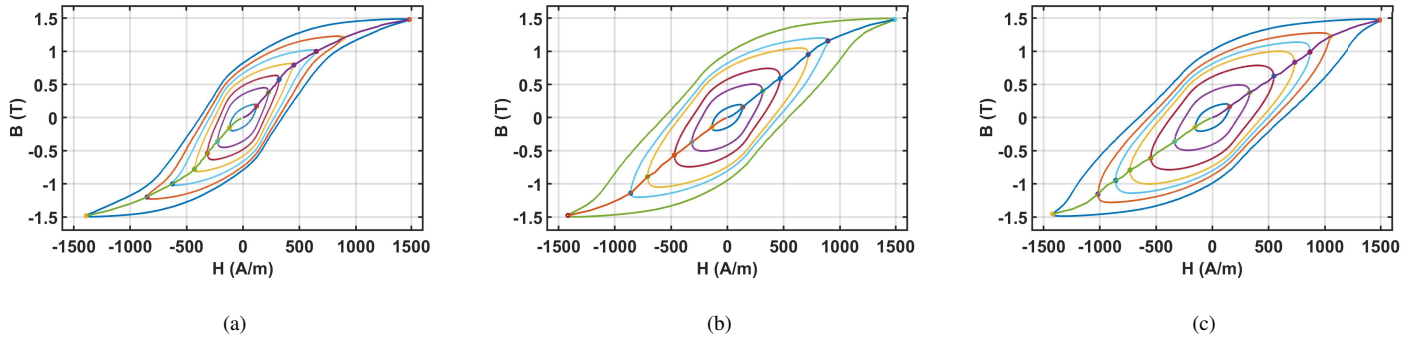


Fig. 4. B-H loops at different B_{max} for 50C600 at (a) 400 Hz (b) 800 Hz (c) 1000 Hz

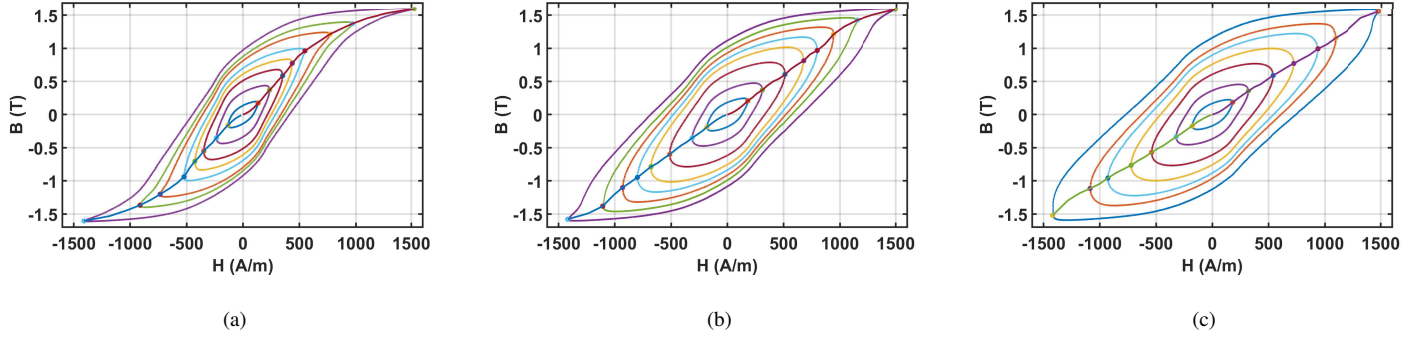


Fig. 5. B-H loops at different B_{max} for 50C800 at (a) 400 Hz (b) 800 Hz (c) 1000 Hz

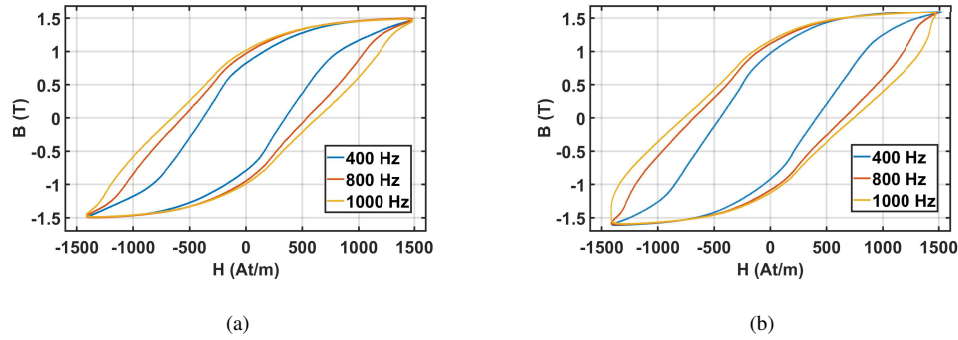


Fig. 6. B-H loops at 400 Hz, 800 Hz, and, 1000 Hz for (a) 50C600 (b) 50C800

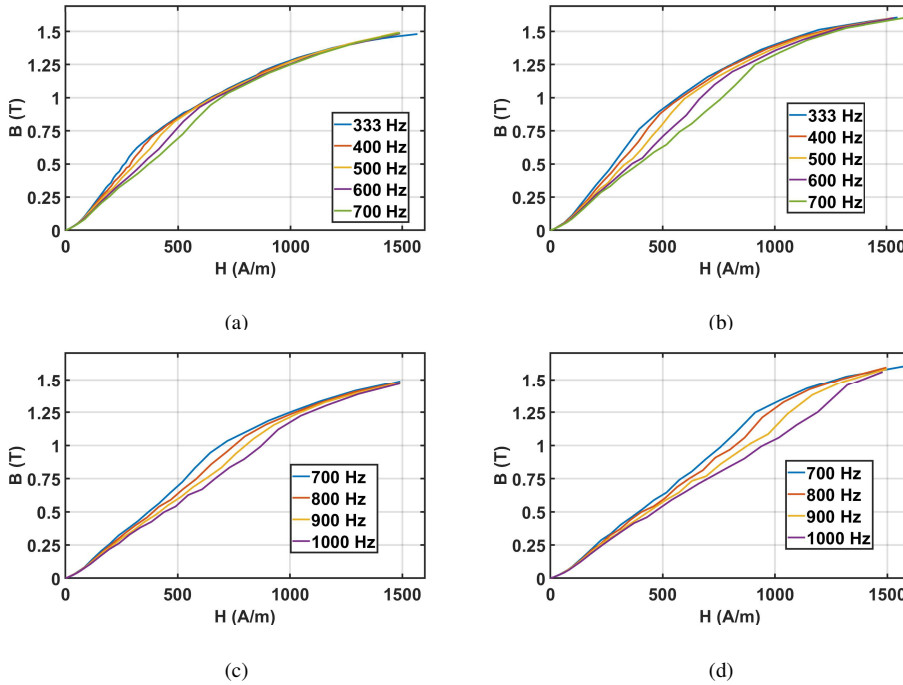


Fig. 7. B-H curves for (a) 50C600, 333 Hz - 700 Hz (b) 50C800, 333 Hz - 700 Hz (c) 50C600, 700 Hz - 1000 Hz (d) 50C800, 700 Hz - 1000 Hz

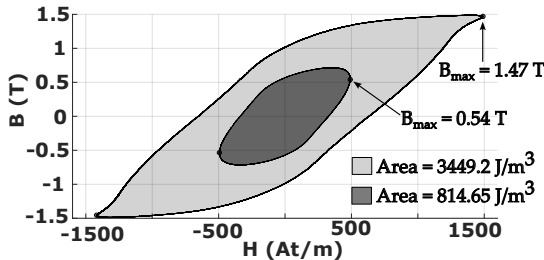


Fig. 8. Illustration for core loss calculation (50C600 at 1 kHz)

814.65 J/m³. A product of this energy loss and the frequency gives the energy loss due to the loop in each second in unit volume of the core material. The power loss thus obtained, is divided with the material mass density to get the specific power loss in terms of W/kg. This procedure is repeated for multiple B-H loops, each corresponding to a particular value of peak flux-density. One more B-H loop shown in Fig. 8 has a peak flux-density of 1.47 T, and a loop area of 3449.2 J/m³. The variation of the obtained power loss with flux-density is plotted. The same procedure is repeated at different frequencies to get a family of core-loss curves for both the materials for the frequency range of 333 Hz to 1000 Hz, as shown in Fig. 9(a)-(d).

The core-loss values at typical operating frequencies and flux-densities are shown in Table- II. 50C600 is denoted by S1, and 50C800 is denoted by S2. It is observed that the core loss for same value of peak flux density is higher at higher frequencies. 50C800 (i.e., S2) is observed to have higher core-loss than 50C600 (i.e., S1) at each frequency. From Fig. 6(a)-(b), it is observed that the loop area increases with fre-

quency. This indicates an increased loss in the magnetization-demagnetization cycle. Further, the core-losses increase more rapidly with frequency at higher values of peak flux-densities.

IV. CONCLUSIONS

In this paper, two SiFe alloys- 50C600 and 50C800 are experimentally characterized for their B-H loops over a frequency range of 333 Hz-1000 Hz and flux-density of around 1.5 T. B-H curves and loss curves at each frequency are thereby obtained. 50C800 is found to have slightly higher permeability upto 800 Hz, but higher core-loss at all frequencies, as compared to 50C600. It is also observed that the core losses at 1.5 T scale up by more than ten times at 400 Hz, as compared to the values for 50 Hz mentioned in the datahsheet. Such experimental results can serve as crucial inputs in the electromagnetic design and performance analysis of high-speed machines made using these materials, and subsequently in the design of thermal systems for such machines.

V. ACKNOWLEDGEMENT

The authors would like to thank TD Power Systems, Bengaluru, India for their help in fabrication of the toroidal cores.

REFERENCES

- [1] J. Z. Bird, "A Review of Electric Aircraft Drivetrain Motor Technology," *IEEE Trans. Mag.*, vol. 58, no. 2, pp. 1-8, Feb. 2022, Art no. 8201108, doi: 10.1109/TMAG.2021.3081719.
- [2] P. Ramesh and N. C. Lenin, "High Power Density Electrical Machines for Electric Vehicles—Comprehensive Review Based on Material Technology," *IEEE Trans. Magn.*, vol. 55, no. 11, pp. 1-21, Nov. 2019, Art no. 0900121, doi: 10.1109/TMAG.2019.2929145.
- [3] E. Sayed et al., "Review of Electric Machines in More-/Hybrid-/Turbo-Electric Aircraft," *IEEE Trans. Transp. Electric.*, vol. 7, no. 4, pp. 2976-3005, Dec. 2021, doi: 10.1109/TTE.2021.3089605.

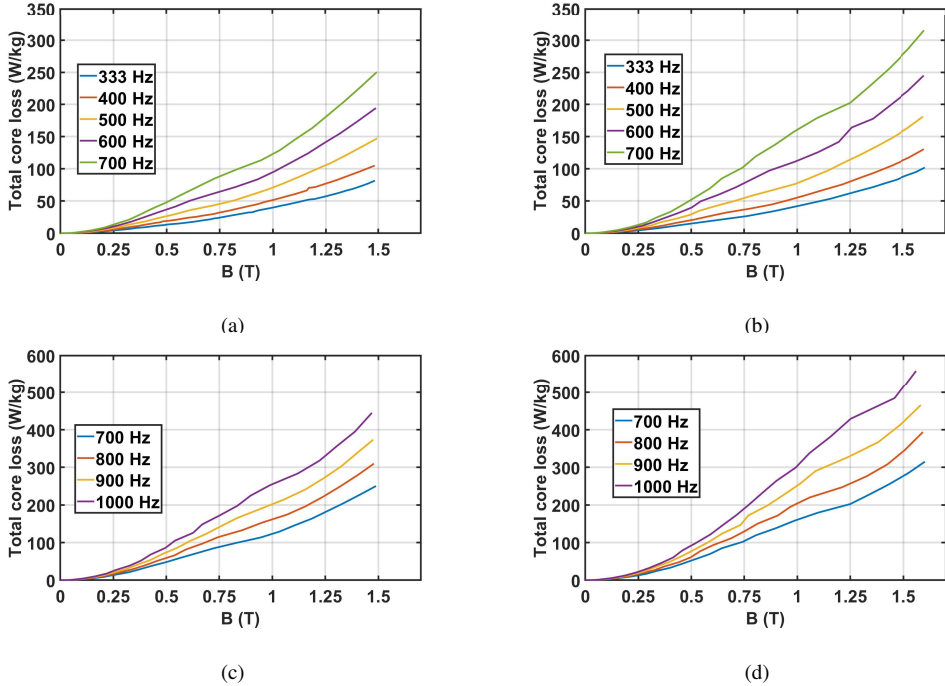


Fig. 9. Core loss curves for (a) 50C600, 333 Hz - 700 Hz (b) 50C800, 333 Hz - 700 Hz (c) 50C600, 700 Hz - 1000 Hz (d) 50C800, 700 Hz - 1000 Hz

TABLE II
COMPARISON OF CORE LOSS IN W/KG FOR 50C600 (S1), 50C800 (S2)

Flux density	400 Hz	600 Hz	800 Hz	1000 Hz
0.53 ± 0.02 T	S1- 21.22, S2- 21.32	S1- 41.26, S2- 49.52	S1- 65.91, S2- 77.08	S1- 105.12, S2- 99.07
0.98 ± 0.03 T	S1- 51.42, S2- 51.6	S1- 96.16, S2- 111.06	S1- 152.9, S2- 195.2	S1- 252.58, S2- 299.56
1.45 ± 0.03 T	S1- 105.06, S2- 105.58	S1- 194.43, S2- 198.11	S1- 309.92, S2- 307.95	S1- 445.06, S2- 484.35

- [4] J. Benzaquen, J. He and B. Mirafzal, "Toward more electric powertrains in aircraft: Technical challenges and advancements," *CES Trans. Elect. Mach. and Syst.*, vol. 5, no. 3, pp. 177-193, Sept. 2021, doi: 10.30941/CESTEMS.2021.00022.
- [5] Y. Wang, S. Nuzzo, H. Zhang, W. Zhao, C. Gerada and M. Galea, "Challenges and Opportunities for Wound Field Synchronous Generators in Future More Electric Aircraft," *IEEE Trans. Transp. Electricif.*, vol. 6, no. 4, pp. 1466-1477, Dec. 2020, doi: 10.1109/TTE.2020.2980189.
- [6] V. Madonna, P. Giangrande and M. Galea, "Electrical Power Generation in Aircraft: Review, Challenges, and Opportunities," *IEEE Trans. Transp. Electricif.*, vol. 4, no. 3, pp. 646-659, Sept. 2018, doi: 10.1109/TTE.2018.2834142.
- [7] J. K. Nøland, M. Leandro, J. A. Suul and M. Molinas, "High-Power Machines and Starter-Generator Topologies for More Electric Aircraft: A Technology Outlook," in *IEEE Access*, vol. 8, pp. 130104-130123, 2020, doi: 10.1109/ACCESS.2020.3007791.
- [8] C. Urabinahatti, S. S. Ahmad and G. Narayanan, "Magnetic Characterization of Ferromagnetic Alloys for High-Speed Electric Machines," *IEEE Trans. Industry Appl.*, vol. 56, no. 6, pp. 6436-6447, Nov.-Dec. 2020, doi: 10.1109/TIA.2020.3023868.
- [9] M. Kacki, M. S. Rytko, J. G. Hayes and C. R. Sullivan, "Measurement Methods for High-Frequency Characterizations of Permeability, Permittivity, and Core Loss of Mn-Zn Ferrite Cores," *IEEE Trans. Power Electron.*, vol. 37, no. 12, pp. 15152-15162, Dec. 2022, doi: 10.1109/TPEL.2022.3189671.
- [10] Electrical Steel Coil : Product Manual, China Steel Corporation India (CSCI), [Online]. Available: https://www.csc.com.tw/csc_e/pdf/CSCI_ES_Catalog.pdf
- [11] A. Krings, M. Cossale, A. Tenconi, J. Soulard, A. Cavagnino and A. Boglietti, "Magnetic Materials Used in Electrical Machines: A Comparison and Selection Guide for Early Machine Design," *IEEE Trans. Industry Appl.*, vol. 23, no. 6, pp. 21-28, Nov.-Dec. 2017, doi: 10.1109/MIAS.2016.2600721.
- [12] A. Krings, A. Boglietti, A. Cavagnino and S. Sprague, "Soft Magnetic Material Status and Trends in Electric Machines," *IEEE Trans. Ind. Electron.*, vol. 64, no. 3, pp. 2405-2414, March 2017, doi: 10.1109/TIE.2016.2613844.
- [13] Soft Magnetic Alloy with High Magnetic Flux Density Permendur [Online]. Available: <https://www.hitachi-metals.co.jp/e/products/infr/ai/permendur.html>
- [14] N. Fernando, G. Vakil, P. Arumugam, E. Amankwah, C. Gerada and S. Bozhko, "Impact of Soft Magnetic Material on Design of High-Speed Permanent-Magnet Machines," *IEEE Trans. Ind. Electron.*, vol. 64, no. 3, pp. 2415-2423, March 2017, doi: 10.1109/TIE.2016.2587815.
- [15] L. K. Rodrigues and G. W. Jewell, "Model Specific Characterization of Soft Magnetic Materials for Core Loss Prediction in Electrical Machines," *IEEE Trans. Magn.*, vol. 50, no. 11, pp. 1-4, Nov. 2014, Art no. 2105204, doi: 10.1109/TMAG.2014.2328099.
- [16] S. S. Ahmad, A. Raj and G. Narayanan, "Low-cost Multistage Direct-Coupled Linear Power Amplifier for Characterization of Magnetic Cores at Multiple Frequencies," *2021 National Power Electronics Conference (NPEC)*, 2021, pp. 1-6, doi: 10.1109/NPEC52100.2021.9672514.
- [17] R. Raj, B. S. Ram, R. Bhat, G. M. Unniachanparambil and S. V. Kulkarni, "A Novel Cost-Effective Magnetic Characterization Tool for Soft Magnetic Materials Used in Electrical Machines," *IEEE Trans. Instrum. Meas.*, vol. 70, pp. 1-8, 2021, Art no. 6009508, doi: 10.1109/TIM.2021.3099558.
- [18] IEC 2003 Methods of measurement of the magnetic properties of magnetically soft metallic and powder materials at frequencies in the range 20 Hz to 200 kHz by use of ring specimens *IEC Standard Publication 60404-6* (Geneva: IEC Central Office)
- [19] Fiorillo, Fausto. (2010). "Measurements of Magnetic Materials". *Metrologia*. 47. S114. 10.1088/0026-1394/47/2/S11.